

Ground-state selection as a four-wave-mixing process

A. Avidan,* Y. Lahini, D. Mandelik, and Y. Silberberg

Department of Physics of Complex Systems, The Weizmann Institute of Science, 76100 Rehovot, Israel

(Received 26 January 2006; published 9 June 2006; corrected 16 June 2006)

We study nonlinear relaxation of the excited state in a system with two levels and a continuum. The process is first simulated in a one-dimensional waveguide array described by the discrete nonlinear Schrödinger equation. The results are interpreted in terms of degenerate four-wave mixing between the eigenmodes and diffraction properties of the array. We also show analytically that the role of the continuum can be played by a third bound state, with linear loss that replaces the diffraction in the continuum. This model enables derivation of the energy transfer rate and other parameters of the process.

DOI: [10.1103/PhysRevA.73.063811](https://doi.org/10.1103/PhysRevA.73.063811)

PACS number(s): 42.65.Sf, 42.65.Wi, 05.45.-a

I. INTRODUCTION

A two level system model underlies the description of some of the most basic phenomena in physics. In a system described by a potential supporting two bound states without any additional interactions, these two bound states are trivially stable. Namely, if initially all the energy is concentrated in one state, no exchange of energy will occur during propagation. Silberberg and Stegeman [1] have studied the effect of Kerr nonlinearity on an optical waveguide supporting two bound states. They showed that the power is exchanged periodically between the two modes, except one critical power at which one mode grows asymptotically. An electromagnetic eigenmode $\varepsilon_n(x,y)e^{i\beta_n z}$ of an isotropic lossless optical waveguide with a refractive index profile $n(x,y)$ is given by the solution of the equation

$$\frac{\partial^2 \varepsilon_n}{\partial x^2} + \frac{\partial^2 \varepsilon_n}{\partial y^2} + (nw/c)^2 \varepsilon_n = \beta_n^2 \varepsilon_n \quad (1)$$

which is completely analogous to the time independent Schrödinger equation, with a potential well proportional to $-n(x,y)^2$, and negative bound state energies proportional to $-\beta_n^2$.

Since in practice all potentials have in addition a spectrum of unbound states or a “continuum,” it is important to examine the changes such states impose on the nonlinear interaction between the different bounded modes. Weinstein and Soffer [2] investigated the nonlinear Schrödinger equation (NLSE) with a *linear* spectrum of two bound states and a *continuum* of unbound states. They considered the nonlinear potential as a small perturbation and showed that the excited state has a characteristic lifetime during which half of the population in it is transferred to the continuum while the other half decays to the ground state. This process ends when the energy at the excited state drops to zero. In this sense we say that the ground state maintains its stability while the excited state does not. From now on we will refer to this process as ground state selection (GSS). In a potential with more than two bound states Skupin *et al.* [3] showed that

bound states failing to fulfill a four-wave mixing criterion are unstable.

Recently Mandelik *et al.* [4], demonstrated the process in an (Al,Ga)As slab waveguide, supporting two confined modes. Their experiment showed that the power in the anti-symmetric mode at the output facet decays, while transferring large amounts of energy to the symmetric mode and to the continuum.

The process of the GSS might be relevant for other nonlinear physical systems supporting a discrete set of bound states. Consider, for example, the collective excitations in cold dilute atom gases, and the formation of Bose-Einstein condensates (see [5]). In the mean field approximation such condensates are described by the Gross-Pitaevskii equation, which is the NLSE supplemented by an unbound potential, that represents the magnetic trap confining the bosons into a condensate. Here a relaxation to the collective excitation ground state can occur while radiating some of the energy.

Since the stability criterion suggested by [3] is phase matching of the four-wave-mixing (FWM) process, it is our intention in this paper to give a simple and intuitive explanation of the GSS based on FWM.

In the first part of this paper we consider the GSS effect in a one-dimensional waveguide array in the presence of a weak Kerr nonlinearity. This system has several numerical advantages which make it suitable for demonstrating the process: Since it is one-dimensional, the computational time is relatively short. With the help of defect manipulation, we can build a linear spectrum appropriate for our cause. For example, we can easily engineer a discrete potential well which will support only two guided modes, while the rest of the extended states can serve as a continuum. This, as will be shown below, results in a spectrum of two bound states and a continuum.

In the second part, we suggest a model that accounts for the different aspects of the GSS traced in the discrete realization. This model is based on degenerate four-wave-mixing (DFWM), where one of the waves experiences a high linear loss. Finally, we discuss the results and compare them to those obtained in the discrete simulation.

II. DISCRETE GSS IN A ONE-DIMENSIONAL WAVEGUIDE ARRAY

In this section we discuss the prominent features of the GSS process in a one-dimensional waveguide array. As was

*Email address: assaf.avidan@weizmann.ac.il

discussed in the introduction, we can create a discrete potential well along the array which supports only two modes which are spatially confined to the vicinity of the well. By correctly choosing the various parameters we can have a spectrum in which the density of states among the extended modes is much higher than the density at the bound states, thus it can be treated as a continuum. We begin with a brief review of the spectrum of a one-dimensional waveguide array.

A one-dimensional waveguide array comprised of N single mode identical waveguides can be described within the coupled mode theory which accounts for the first band of the array's spectrum [6]. In the presence of weak Kerr nonlinearity, the envelope of the electromagnetic field in the m th waveguide is described by the discrete nonlinear Schrödinger equation (DNLS)

$$i \frac{dE_m}{dz} = \beta_0 E_m + c_{m,m-1} E_{m-1} + c_{m,m+1} E_{m+1} + \gamma |E_m|^2 E_m. \quad (2)$$

Here β_0 is the propagation constant of a single waveguide, given by $\beta_0 = 2\pi n/\lambda$, where n is the refractive index in each waveguide, λ is the wavelength, $c_{n,m}$ is the linear coupling constant between the n th and m th waveguides, z is the propagation distance, and $\gamma = \omega n_2^2 / (c A_{eff})$, where n_2 , A_{eff} , ω , and c are the Kerr nonlinearity coefficient, effective area of the a single waveguide mode, the field frequency, and the speed of light, respectively. If $c_{m,m+1}$ is the same for all waveguides and is given by C , then the r th eigenmode of the linear part of Eq. (2) can be written as $\alpha A_r e^{ik_r z - i\beta_r z}$, and β_r is given by the diffraction relation

$$\beta_r = \beta_0 + 2C \cos(ak_r) \quad (3)$$

where a is the lattice constant and k_r is confined to the first Brillouin zone $k_r = 2r\pi/Na$, $-N/2 < r \leq N/2$.

There are several useful ways to manipulate the array's spectrum. For example, changing the number of waveguides and/or the specific value of the coupling constants changes the spectral density of states, and the diffraction properties of the array. Here we create a discrete potential well by choosing four waveguides, and rising the coupling constant in between them.

Figure 1 shows the linear spectrum of an array with $N=1801$ waveguides, and coupling constant defects around the central waveguide

$$C_{m,m+1} = C_{def} \quad m = 899, 901, 902, 903 \quad (4)$$

$$C_{m,m+1} = C \quad m \neq 899, 901, 902, 903. \quad (5)$$

Because the defects create a structure of four waveguides which have higher coupling constants than the rest of the array, there will be two sets of isolated bound/defect states, an unstaggered set, which includes the propagation constants β_1 and β_2 , and a staggered set which includes α_1 and α_2 . The solid line in Fig. 1 represents the area in which the density of states is much higher than at the edges of the spectrum, and we refer to this part of the spectrum as the continuum. Note that each set has phase matched continuum levels α_3 and β_3 ,

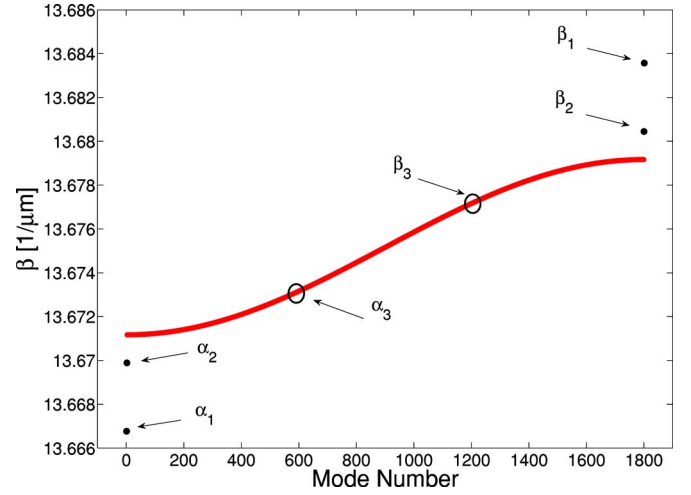


FIG. 1. (Color online) Linear spectrum of a 1801 WGA with coupling constant defects around the center. The horizontal axis is the mode number and the vertical axis represents the eigenvalues β_r . Note the existence of phase matched continuum states β_3 and α_3 . We used the following values: $C_{def}=2.4C$, $C=2000$ 1/m, $\lambda=1.53$ μm , $n=3.33$.

surrounded by nearly phased matched modes. The propagation constants of the phased matched states satisfy the following phase matching condition [3]:

$$\beta_2 - \beta_1 = \beta_3 - \beta_2, \quad \alpha_2 - \alpha_1 = \alpha_3 - \alpha_2. \quad (6)$$

In Fig. 2 we present the power evolution of the two unstaggered bound states, which was obtained by simulating Eq. (2), using the waveguide array parameters given under Fig. 1. The initial conditions are such that 80% of the power is in the excited state, and the rest is in the ground state. As long as

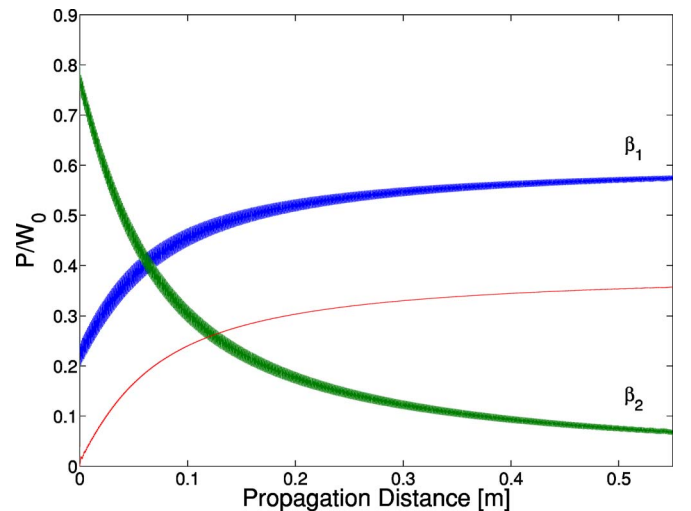


FIG. 2. (Color online) Power exchange between the two bound states. The x axis is the propagation distance, and the y axis is the power in each mode normalized by the initial total power P_0 . At the beginning of the propagation 80% of the total power is in the β_2 state, while 20% is in the β_1 state. The thin line represents the buildup of the continuum modes. We used the following values: $\gamma=5.4$ W/m, $W_0 = \sum_{n=1}^N |E_n|^2 = 500$ W.

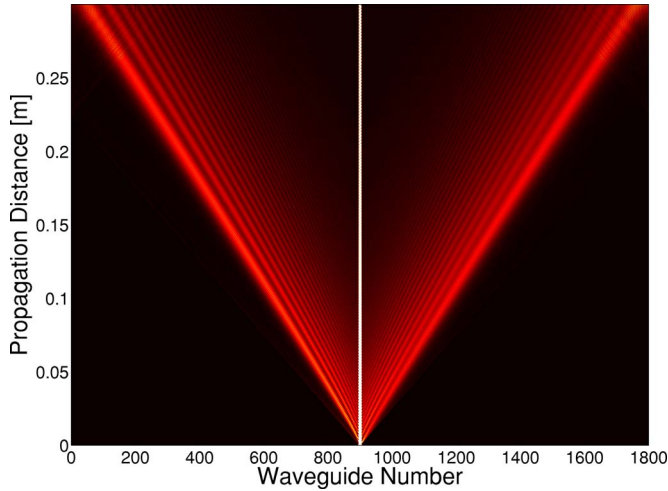


FIG. 3. (Color online) A color map view of the radiation modes diffracted away from the defect zone, which appears as a straight white line in the figure.

at the beginning there was a fraction of the power in the exited mode, the qualitative behavior we observed was the same.

The thick lines in Fig. 2 are the result of nonlinear oscillations between the two bound states. The power in the mode with the propagation constant β_2 (β_1), is decreasing (increasing) on a distance scale which is much larger than the scale of oscillations in each mode. The system reaches a steady state in which half of the initial power of β_2 decays to β_1 , while the other half is released to the unbound states of the spectrum, i.e., to the continuum. We verified that this asymptotic behavior is stable and does not depend on the initial conditions. For example, if all the initial power is placed in β_1 then no exchange of energy will occur during the propagation, and the system will stay in its initial state. In this sense we say that the system selects the β_1 mode as its nonlinear ground state [2].

In the simulation, we found out that the propagation distance scales inversely with the initial total power squared, for example increasing the propagation distance by four and decreasing the initial power by two leads to the same result. We also observed that the propagation distance scales linearly with the inverse of the coupling constant C , (and C_{def} is a fixed proportion of C). In order to keep the discussion in the weak nonlinear regime, we made sure that $\gamma|E_n|^2/C$ reaches the maximal value of 0.2 at the beginning of the propagation, and drops below 0.03 towards the end. A color map view is given in Fig. 3. The power in each waveguide is plotted as a function of the propagation distance. Due to the diffraction properties of the first band [7], waves which are released to the continuum travels at an angle with respect to the horizontal axis in Fig. 3, thus diffract away from the defect area. The above mechanism is not unique to the discrete case. For example, bound states evolving in time will radiate energy to the continuum. This energy will *disperse*, and in a complete analogy to the discrete case, will no longer take part in the process.

A further insight into the process is obtained by an examination of the continuum level spectrum. Since the nonlinear-

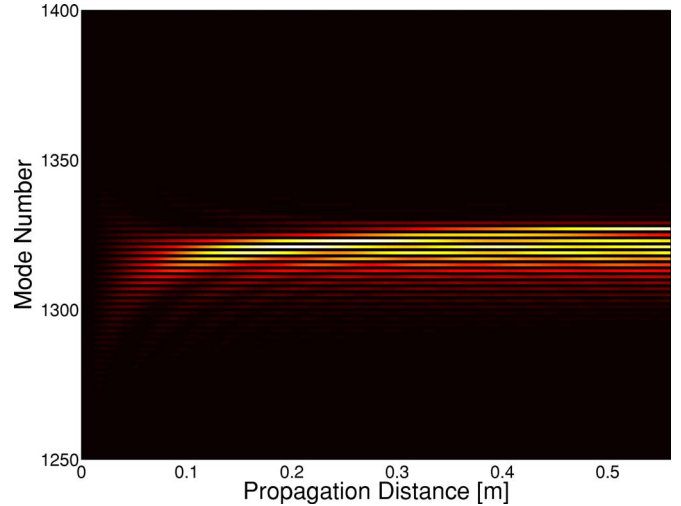


FIG. 4. (Color online) GSS continuous spectrum. A finite width mini band is created in the continuum as a result of slightly non-phased matched terms participating in the FWM.

ity is weak, a band of nonlinear bound states emanates from each of the two linear bound states [3]. If the density of states in the continuum is high enough, slightly nonphase matched states can also participate in the DFWM, creating a *mini band* centered at β_{mb} within the continuous spectrum. In Fig. 4 we plot a color map of the power as a function of both the continuum level and the propagation distance. Comparing the center of the mini band to what is predicted by Eq. (6) we find that $\beta_{mb}/\beta_3 \approx 1.2$. The small mismatch is due to the different nonlinear spectral shifts acquired by the two bound states. We verified numerically that the smaller the nonlinear deformation of the bound states is, the smaller the mismatch.

It is interesting to note that the staggered bound states also show GSS similarly to the unstaggered states, but with one important difference. In the staggered case the system selects the mode with the lowest propagation constant (α_1 in Fig. 1) as its nonlinear ground state, as opposed to the unstaggered case where the selected ground state is the mode with the highest propagation constant. This situation is the same for two level systems in which the discrete modes are characterized by different energies rather than different propagation constants. In such a case the staggered nonlinear ground state will be the bound state with the *higher* energy.

III. FOUR-WAVE-MIXING MODEL

It is our intention in this section to give an analytic description of the GSS based on the above results. Equation (6) motivates us to explain the results presented in Fig. 2 in terms of degenerate four-wave mixing (DFWM) of photons. Equation (6) suggests that each pair of β_1 and β_3 photons turns into a pair of β_2 photons and vice versa. Since the mini band has a finite width, photons in the continuum level quickly diffract across the array, and no longer participate in the DFWM process. For each β_3 photon which is lost by diffraction, there is a one photon gain in the β_1 level, which is also no longer a part of the DFWM. This process will end

once β_3 and β_2 are both empty, leaving in the state β_1 half of the initial β_2 population. To start the analytic description of the GSS, we consider the propagation equation of a single frequency field w in an isotropic Kerr nonlinear medium, with refractive index $n(x, y)$ which supports *three* transverse electromagnetic linear modes, (in MKS units)

$$\nabla^2 E + (nw/c)^2 E = -\mu\chi w^2 |E|^2 E, \quad (7)$$

where μ is the matter permeability, c the velocity of light in vacuum, and χ the third order nonlinear susceptibility. We denote the propagation constant of the i th mode and the propagation direction by β_i and z , respectively, so that the three linear modes take the form

$$E_i = \varepsilon_i(x, y) \exp i\beta_i z \quad i = 0, 1, 2. \quad (8)$$

For simplicity we take $\varepsilon_i(x, y)$ to be real valued functions. Although in this section we investigate Eq. (7), the exact same analysis performed below can be applied both to NLSE and DNLSE equations, and the results of this section will hold, specifically Eq. (17). The normalization of the linear modes is chosen so that each mode corresponds to a power of S [Watt]. The linear modes then satisfy the orthogonality relation [6] $\frac{\beta_i}{w\mu} \int_{-\infty}^{\infty} \int_{-\infty}^{\infty} \varepsilon_i \varepsilon_j dx dy = S \delta_{ij}$. In addition, since we want to use FWM arguments, we postulate that the three linear modes satisfy Eq. (6). Assuming the propagation is described as a super position of these three modes, and using the slowly varying amplitude approximation, Eq. (7) yields equations for the evolution of the complex coefficients A_i with z . Taking into account only phase matched terms, and defining $A_i = u_i e^{i\phi_i}$ and $\theta = 2\phi_1 - \phi_0 - \phi_2$, the equations of motion read

$$\frac{dU_0}{dZ} = \frac{1}{2} U_1^2 U_2 \sin \theta, \quad (9)$$

$$\frac{dU_1}{dZ} = -U_0 U_1 U_2 \sin \theta, \quad (10)$$

$$\frac{dU_2}{dZ} = \frac{1}{2} U_1^2 U_0 \sin \theta. \quad (11)$$

$$-\frac{d\theta}{dZ} = B_0 U_0^2 + B_1 U_1^2 + B_2 U_2^2 + \cos \theta \left[2U_2 U_0 - \frac{U_2 U_1^2}{2U_0} - \frac{U_0 U_1^2}{2U_2} \right]. \quad (12)$$

We used the normalization $Z = zBW$, $U_i = u_i / \sqrt{W}$, and the definitions $B = b_{0112}$, $B_1 = (2b_{1111} - b_{0011} - b_{1122})/B$, $B_2 = (2b_{1111} - b_{0011} - b_{1122})/B$, $B_0 = (2b_{1122} - \frac{1}{2}b_{2222} - b_{0022})/B$, where for simplicity we assumed that $B > 0$. Here $W = 2u_0^2 + u_1^2$ is a constant of motion and the notation b_{ijk} stands for the integrals

$$b_{ijk} = \frac{1}{2S} w\chi \int_{-\infty}^{\infty} \int_{-\infty}^{\infty} \varepsilon_i \varepsilon_j \varepsilon_k dx dy. \quad (13)$$

We also assumed that $u_0, u_2 \neq 0$, which means that our system is in a mixed state so that not all the energy is con-

centrated in one bound state. Note that, due to our normalization, U_0^2 takes the values between 0 and $\frac{1}{2}$ and U_1^2 takes the values between 0 and 1.

We now need to include the effect of radiation of the continuum level in the GSS process. For that we add a linear loss term $-\Gamma U_2$ to Eq. (11), where Γ is a positive constant. Equation (11) now takes the form

$$\frac{dU_2}{dZ} = \frac{1}{2} U_1^2 U_0 \sin \theta - \Gamma U_2. \quad (14)$$

The most important assumption we make in order to solve Eqs. (9)–(12) is to take the flows of energy in and out of the β_2 state to be equal, so that U_2 is in a kind of steady state. Mathematically this can be put by $dU_2/dZ \ll \Gamma U_2$, and $dU_2/dZ \ll U_1^2 U_0 \sin \theta$. Following that, an expression for U_2 is immediately obtained,

$$U_2 = \frac{U_1^2 U_0 \sin \theta}{2\Gamma}. \quad (15)$$

Plugging Eq. (15) into Eq. (12) and taking the limit $\Gamma \gg \max(1, B)$, we can keep only terms proportional to Γ . If we assume $\cos \theta|_{z=0} \neq 0$ we may solve for θ

$$\cos \theta = \cos \theta|_{z=0} e^{-\Gamma Z}. \quad (16)$$

This solution implies that after a propagation distance of $1/\Gamma$, the phase approaches the value of $\pi/2$. For intermediate values of γ , stability analysis shows that there is a steady state solution for $\cos(\theta)$ different from zero, which approaches zero as γ goes to infinity. Using this result, Eqs. (9) and (10) turn into

$$\frac{dP_0}{dZ} = \frac{P_1^2 P_0}{2\Gamma}$$

$$\frac{dP_1}{dZ} = -\frac{P_1^2 P_0}{\Gamma}, \quad (17)$$

where $P_i = U_i^2$. Equations (16) and (17) show that the scale on which $\cos \theta$ changes is $1/\Gamma$ while the scale on which P_i changes is Γ , so that taking the limit of large Γ separates the two scales. This means that for large enough Γ , the phase is locked on $\pi/2$ before there is any significant change in P_0, P_1 . The same result was obtained by Weinstein and Soffer [2] who used a multi time scale analysis to study the NLSE with a spectrum including two bound states and a continuum. They proved rigorously that the solution decomposes into three time scales, the last of which is given by Eqs. (17), and that $1/\Gamma$ can be calculated by the nonlinear Fermi golden rule.

A stability analysis based on phase space arguments [8], shows that $P_0 = 1/2, P_1 = 0$ is the only stable steady state solution of Eq. (17). Thus for long enough propagation

$$P_0(\infty) \rightarrow \frac{1}{2}$$

and, as a consequence,

$$P_1(\infty) \rightarrow 0. \quad (18)$$

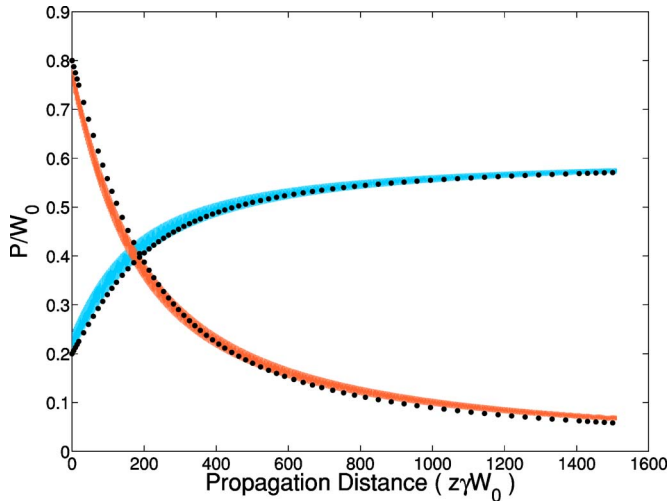


FIG. 5. (Color online) Direct comparison between the results obtained from the discrete simulation, and the DFWM model. The dotted lines are the solution of Eq. (17).

Alternatively, in terms of initial conditions,

$$\frac{P_0(\infty) - P_0(0)}{P_1(0)} = \frac{1}{2}. \quad (19)$$

The above steady solution shows that the P_1 state is *unstable*. Moreover, it will hold for any initial conditions, provided that $U_0(Z=0) \neq 0$ $i=1,2$. In particular, the result of a perturbation of the U_0 state will be the same as Eq. (18), i.e., the U_0 state is *stable*.

We would like to test Eqs. (17) on the discrete numerical case studied in Sec. II. There, we engineered a discrete potential well which has only two bound states, and used the rest of the extended modes as a continuum. In the analysis of Sec. II we assumed that P_2 receives energy from P_1 through a DFWM process, and immediately loses it. From Eqs. (17) we see that the rate at which energy is transferred from P_1 to P_0 and P_2 is given by $(BW)/\Gamma$. However, in the discrete simulation we know that the inverse of the mini-band width

$\delta[1/m]$, gives the rate at which the continuum levels build up. The above suggests that, in order to use Eqs. (17) for the discrete simulation, we should take $\delta = \gamma W_0/\Gamma$, where instead of W we used the normalization of the discrete simulation $W_0 = u_0(0)^2 + u_1(0)^2 + u_2(0)^2$, and we switched B with the discrete nonlinear susceptibility γ .

Indeed, the number of modes in the mini band is about six, multiplying by the width of a single mode $4C/N$, we get the width of the miniband $\delta = 24C/N$. For the discrete case $\Gamma = \gamma W_0/\delta$, or $\Gamma = \gamma W_0 N/24C$, which is proportional to the inverse of the coupling constant, which is exactly as predicted in Sec. II. Plugging in the numbers, we find $\Gamma \approx 100$. Scaling the distance in Eq. (2) to match the scaling of Eq. (17), and normalizing u_i^2 with W_0 instead of W , we can make a direct comparison between the two results. In Fig. 5 we present the rescaled data from Fig. 2 which appears again as thick lines in the figure. On top we plot the solution of Eqs. (17), calculated with the value $\Gamma = 100$. Figure 5 shows that the results of our analysis fit the discrete simulation well.

IV. DISCUSSION

Based on the results we obtained from the discrete simulation, we presented a DFWM model of the GSS. We showed that we can account for diffraction in the continuum by adding a large enough loss term to one of the guided modes. As a result we obtained an integrable set of equations, with a decay rate $(WB)^2/\alpha$, where α is the unscaled loss parameter, which from dimensional analysis is proportional to the diffraction length in the continuum. We found that P_0 is *stable*, whereas the P_1 state is *unstable*. If we choose to damp P_0 instead, P_2 becomes the stable ground state, although it has the highest propagation constant, similar to the staggered GSS. In addition we demonstrated that the decay rate can be calculated once the width of the continuum miniband is known, and used this result to show that Eqs. (17) describe the discrete case well. To complete the discussion, we remark that the presence of a mini band embedded in the continuum is possible only if the level spacing ($|\beta_1 - \beta_2|$) is large enough. In cases where the phased matched miniband is placed outside the continuous spectrum, our picture fails and the description given in [1] is valid.

- [1] Y. Silberberg and G. I. Stegeman, Appl. Phys. Lett. **50**, 13,801 (1987).
 [2] A. Soffer and M. I. Weinstein, Phys. Rev. Lett. **95**, 213905 (2005).
 [3] S. Skupin, U. Peschel, L. Berge, and F. Lederer, Phys. Rev. E **70**, 016614 (2005).
 [4] D. Mandelik, Y. Lahini, and Y. Silberberg, Phys. Rev. Lett. **95**, 073902 (2005).

- [5] D. S. Jin, J. R. Ensher, M. R. Matthews, C. E. Wieman, and E. A. Cornell, Phys. Rev. Lett. **77**, 420 (1996).
 [6] A. Yariv, *Optical Waves in Crystals* (Wiley, New York, 1984).
 [7] F. Lederer and Y. Silberberg, Opt. Photonics News **13**, 48 (2002).
 [8] S. H. Strogatz, *Nonlinear Dynamics and Chaos* (Addison-Wesley, Reading, MA, 1994).